Ecology and Evolution

The relationship of leaf photosynthetic traits – V_{cmax} and J_{max} – to leaf nitrogen, leaf phosphorus, and specific leaf area: a meta-analysis and modeling study

Anthony P. Walker[1,2], Andrew P. Beckerman[1], Lianhong Gu[2], Jens Kattge[3], Lucas A. Cernusak[4], Tomas F. Domingues[5], Joanna C. Scales[6], Georg Wohlfahrt[7], Stan D. Wullschleger[2] & F. Ian Woodward[1]

[1]Department of Animal and Plant Sciences, University of Sheffield, Alfred Denny Building, Western Bank, Sheffield S10 2TN, UK
[2]Environmental Sciences Division, Climate Change Science Institute, Oak Ridge National Laboratory, Oak Ridge, Tennessee 37831-6301
[3]Max Plank Institute for Biogeochemistry, Jena, Germany
[4]Department of Marine and Tropical Biology Cairns, James Cook University, Cairns, Queensland 4878, Australia
[5]Depto. de Biologia, Faculdade de Filosofia, Ciências e Letras de Ribeirão Preto, Av. Bandeirantes, 3900 – CEP 14040-901, Ribeirão Preto, Brasil
[6]Plant Biology and Crop Science, Rothamsted Research, Harpenden, Herts, AL5 2JQ, UK
[7]University of Innsbruck, Institute of Ecology, Sternwartestrasse 15, 6020 Innsbruck, Austria

Abstract

Great uncertainty exists in the global exchange of carbon between the atmosphere and the terrestrial biosphere. An important source of this uncertainty lies in the dependency of photosynthesis on the maximum rate of carboxylation (V_{cmax}) and the maximum rate of electron transport (J_{max}). Understanding and making accurate prediction of C fluxes thus requires accurate characterization of these rates and their relationship with plant nutrient status over large geographic scales. Plant nutrient status is indicated by the traits: leaf nitrogen (N), leaf phosphorus (P), and specific leaf area (SLA). Correlations between V_{cmax} and J_{max} and leaf nitrogen (N) are typically derived from local to global scales, while correlations with leaf phosphorus (P) and specific leaf area (SLA) have typically been derived at a local scale. Thus, there is no global-scale relationship between V_{cmax} and J_{max} and P or SLA limiting the ability of global-scale carbon flux models do not account for P or SLA. We gathered published data from 24 studies to reveal global relationships of V_{cmax} and J_{max} with leaf N, P, and SLA. V_{cmax} was strongly related to leaf N, and increasing leaf P substantially increased the sensitivity of V_{cmax} to leaf N. J_{max} was strongly related to V_{cmax}, and neither leaf N, P, or SLA had a substantial impact on the relationship. Although more data are needed to expand the applicability of the relationship, we show leaf P is a globally important determinant of photosynthetic rates. In a model of photosynthesis, we showed that at high leaf N (3 gm^{-2}), increasing leaf P from 0.05 to 0.22 gm^{-2} nearly doubled assimilation rates. Finally, we show that plants may employ a conservative strategy of J_{max} to V_{cmax} coordination that restricts photoinhibition when carboxylation is limiting at the expense of maximizing photosynthetic rates when light is limiting.

Introduction

Photosynthesis is the proximal driver of the carbon cycle (Canadell et al. 2007; Cadule et al. 2010) and is thus a core driver of carbon flux and central to carbon cycle models (e.g., Woodward et al. 1995; Cox 2001; Sitch et al. 2003; Zaehle and Friend 2010; Bonan et al. 2011). Enzyme kinetic models of leaf photosynthesis (Farquhar et al. 1980; described below) are typically embedded in global carbon cycle models to mechanistically reflect plant physiological responses to atmospheric CO_2. The Farquhar et al. (1980) photosynthetic submodel and its subsequent variants (Von Caemmerer and Farquhar 1981; Farquhar and Wong 1984; Collatz et al. 1991; Harley et al. 1992) are at the heart of almost all land surface models of carbon flux, several ecosystem dynamic models, and dynamic global vegetation models. We hereafter refer to these global land surface, ecosystem, and vegetation models as terrestrial biosphere models (TBMs).

Simulated photosynthetic rates in TBMs are highly sensitive to V_{cmax} and J_{max} (Zaehle et al. 2005; Bonan et al. 2011; Verheijen et al. 2012), the maximum rate parameters of enzyme kinetic processes driving photosynthesis. Accuracy in these parameters is central to an effective photosynthetic submodel in the TBMs. Theory and empirical data suggest that these photosynthetic rates scale with leaf nitrogen (N) via the large amount of leaf N invested in the ribulose 1-5-bisphosphate oxygenase/carboxylase (RuBisCO) protein, and phosphorus (P) availability influences many aspects of plant physiology central to photosynthesis, including membrane solubility, ATP, and NADPH production (Marschner 1995; Taiz and Zeiger 2010). V_{cmax} and J_{max} have also been linked to structural leaf traits via specific leaf area (SLA). Theory and data (Kattge et al. 2009; Domingues et al. 2010; Cernusak et al. 2011) clearly suggest mechanistic links between V_{cmax}, J_{max}, and several functional plant traits that correlate with photosynthetic biochemistry.

Accurate simulation of plant physiological responses to atmospheric CO_2 in TBMs thus requires data on how V_{cmax} and J_{max} scale with plant traits N, P, and SLA accounting for the immense species-specific and regional variation in availability of N and P and subsequent variation in leaf N, P, and SLA.

Here, we provide a global assessment of the relationship between V_{cmax} and J_{max} and leaf N, P, and SLA, drawing on estimates made on 356 species around the world.

When do V_{cmax} and J_{max} variation matter?

TBMs typically assign a single, fixed V_{cmax} or J_{max} parameter value (Rogers 2014) to each plant functional type (PFT). Scaling from plant to ecosystem or globe is achieved via PFT distribution maps. Recently, however, the predictive performance of such models has improved by allowing parameter values to vary. For example, at sites of the FLUXNET network where high-resolution data exist on all parameters and rates, predictive performance improved when V_{cmax} and J_{max} were allowed to vary interannually (Groenendijk et al. 2011). Additionally, some TBMs improve prediction by simulating leaf nitrogen as part of the model and specify a linear relationship between V_{cmax} and leaf N (e.g., Woodward et al. 1995), defined for each PFT (Kattge et al. 2009). Finally, Mercado et al. (2011) demonstrated considerable improvements to model predictions of carbon fluxes in the Amazon when leaf P was taken into account.

Empirically, there is also a strong relationship between J_{max} and V_{cmax} (Wullschleger 1993; Beerling and Quick 1995), and most TBMs simulate J_{max} as a linear function of V_{cmax}. However, this assumption could be erroneous because the correlation between J_{max} and V_{cmax} is likely to be influenced by leaf N, P, and SLA. The coordination hypothesis of photosynthetic resource allocation (Chen et al. 1993) states that the Calvin–Benson cycle limited rate of assimilation (W_c, see below) equals the electron transport-limited rate of assimilation (W_j). The relationship between J_{max} and V_{cmax} affects the relationship between W_c and W_j and may reflect coordination of these two rate-limiting biochemical cycles. When carboxylation is limiting photosynthesis, high investment in J_{max} relative to V_{cmax} would lead to electron transport not used in photosynthesis requiring dissipation of that energy to avoid photoinhibition (Powles 1984; Krause et al. 2012). However, when light is limiting photosynthesis, high investment in J_{max} relative to V_{cmax} would maximize photosynthetic rates. Therefore, a trade-off exists in high investment in J_{max} relative to V_{cmax} whereby the marginal benefit to photosynthetic rates when light is limiting is offset by the cost of energy dissipation when carboxylation is limiting.

Moving forward: global variation in V_{cmax} and J_{max} as a function of N, P, and SLA

As noted above, we make here a global assessment of the relationship between V_{cmax} and J_{max} and leaf N, P, and SLA, drawing on estimates made on 356 species by treatment combinations around the world from 24 different studies. We used these data to test several hypotheses. First, we hypothesized that leaf P will modify the relationship of V_{cmax} to leaf N. Second, we hypothesized that leaf P will modify the relationship of J_{max} to V_{cmax}. Third, drawing on the coordination hypothesis of photosynthetic resource allocation, we predict that the relationship between J_{max} and V_{cmax} results from efficient resource

investment in J_{max} reflecting the trade-off between photosynthetic gain and costs of energy dissipation.

To test our hypotheses, we combine a global meta-analysis of the relationships of V_{cmax} and J_{max} with N, P, and SLA and then examine the consequences of these patterns in a leaf photosynthesis model. Combined, our effort offers a global-scale definition of V_{cmax} and J_{max} variation in relation to leaf-trait variation and provides an empirical alternative to single value PFT scaling or the type of tuned relationships presented above in global TBMs. Our empirical representation of V_{cmax} and J_{max} should lead to improved simulation of carbon fluxes across multiple scales.

Materials and Methods

Literature review & data collection

In September 2012, we searched the Thompson Reuters Web of Science database for "photosynthesis" or "carboxylation" and either "N," "P," or "SLA" and similar related search terms. The aim was to find papers that had simultaneously measured as many of the following leaf traits: V_{cmax}, J_{max}, leaf N, leaf P, and specific leaf area (SLA) or leaf mass-to-area ratio (LMA). Data were copied from tables or digitized from graphics using Grab It! (Datatrend Software 2008). Minimum requirements for inclusion in this study were that either V_{cmax} or J_{max} were calculated from A/C$_i$ curves along with two of the other three leaf traits, yielding data from 24 papers and 135 species x location combinations, distributed globally (Tables 1 and S1). Some of these data were collected on plants in their natural environment and subject to natural environmental variation, while other data were collected on laboratory-grown plants (mostly tree species) subjected to experimental treatments. The majority of the species used in the greenhouses and laboratories were native to the area of the research center. Either species means or treatment means were collected leading to a dataset of 356 species/treatment combinations. The data can be downloaded from the ORNL DAAC (http://dx.doi.org/10.3334/ORNLDAAC/1224).

V_{cmax} and J_{max} are calculated by fitting equations 1 and 2, or 1,3, and 4 to sections of the A/C$_i$ curve (Von Caemmerer and Farquhar 1981; Sharkey et al. 2007), and these calculations are sensitive to the kinetic parameters, K_c and K_o and to Γ_*, used in the fitting process (Medlyn et al. 2002). Using a method (detailed in Appendix S1) similar to Kattge and Knorr (2007), we removed the variation in V_{cmax} and J_{max} across studies caused by different parametric assumptions by standardizing V_{cmax} and J_{max} to a common set of kinetic parameters (derived by Bernacchi et al. 2001). We also corrected V_{cmax} and J_{max} to a com-

mon measurement temperature of 25°C and to the O$_2$ partial pressure at the measurement elevation. Errors introduced by the standardization were well within the measurement error of A/C$_i$ curves (Appendix S2). Standardizing for the kinetic parameters had a substantial impact on V_{cmax} and to a lesser extent J_{max} (Figure S1), as observed by Kattge et al. (2009). Standardization for O$_2$ partial pressure decreases with altitude had a small impact on values taken from plants growing at altitudes up to 2000 m (Figure S2).

We related J_{max} and V_{cmax} such that:

$$\ln(J_{max}) = a_{jv} + b_{jv}\ln(V_{cmax}) \tag{1}$$

where b_{jv} is the slope of the relationship and a_{jv} the intercept. Gu et al. (2010) demonstrated a method-specific bias on b_{jv} (on non-log-transformed variables) caused by predetermination of the limitation state of points on the A/C$_i$. However, most authors in this meta-analysis used a fitting procedure which removed points that were potentially either limitation state (Wullschleger 1993; Sharkey et al. 2007) which minimizes potential biases in b_{jv}.

Where LMA was reported, we converted to SLA by taking the reciprocal of LMA. While this introduced some error (the reciprocal of the mean of a set of values does not equal the mean of the reciprocals of that set), the error was distributed across the whole range of SLA so was unlikely to have biased the effect of SLA. To compare the J_{max} to V_{cmax} relationship from our dataset, we also used V_{cmax} and J_{max} data from Wullschleger (1993) and the TRY database (Kattge et al. 2011; data from Atkin et al. 1997; Kattge et al. 2009). V_{cmax} and J_{max} are measured on a leaf area basis, and in models of photosynthesis, area-based measurement integrates these parameters with light capture. Therefore, we restricted our analysis to leaf-area-based measurements.

Statistical analysis

To assess the importance of P and SLA as covariates with leaf N in determining V_{cmax} and J_{max}, we developed multiple regressions of V_{cmax} or J_{max} as the dependent variable and leaf N, leaf P, and SLA as the independent variables. To increase sample size and increase the range of each variable, we also developed multiple regressions of V_{cmax} or J_{max} against leaf N and either SLA or leaf P. In the analysis of J_{max}, we also included V_{cmax} as an independent variable based on our hypothesis that W_c and W_j are coordinated via the J_{max} to V_{cmax} relationship. We used linear mixed-model regression framework with leaf traits as fixed effects and the author of the paper from which the data were collected as the random effect (Ordonez et al. 2009). Including the study author as a random effect in the regression model accounted for the nonindependence of data within a

study. We were unable to account for differential accuracy between studies, often measured by sampling variance or sample size in meta-analysis, and therefore did not weight the data. All variables were natural-log-transformed to ensure normality of residuals.

Similar to all meta-analyses (Gurevitch and Hedges 1999), there is likely to be some error introduced by the different methods used by the different research groups, but the standardization method and the mixed-model analysis with study group as the random effect will have minimized this error.

All statistical analyses were carried out using the open-source software package R, version 2.13.0 (R Core Development Team 2011). We employed a backward, stepwise, AIC-based model simplification process. Our maximal models contained 3-way interactions for V_{cmax} (and all 2-way interactions in the models with two independent variables) and J_{max} and were fit with the "lme" function of the "nlme" library (Pinheiro et al. 2011). Models were then simplified using the "dropterm" function of the "MASS" library to conserve marginality (see Venables and Ripley 2002). Model selection aimed to find the minimum adequate model – the model explaining the most variation in the dependent variable with minimum necessary parameters. Model selection was based on the model with the lowest corrected Akaike information criterion (AICc) and with a significance level of each model term of $P < 0.1$, subject to conservation of marginality. The AIC is a relative measure of competing models' likelihood penalized by the number of parameters fit by the model, and the AICc is the AIC when corrected for finite sample size (Burnham and Anderson 2002). Given a set of competing models, the model with the lowest AICc can be considered the preferred model (the minimum adequate model).

We report the likelihood ratio test (LRT) statistic between a model and an intercept only (i.e., only random effects) null model and calculated model significance P-values using the chi-square distribution. As there is no mixed-model method to estimate variance in the dependent variable explained by the model, we report the proportional decrease in the residual variance in the minimum adequate model compared with the null, random effects only, model as a metric of explained variance (Xu 2003).

Models were checked for violation of the assumptions of mixed-model linear regression (homoscedasticity of residuals; normal distribution of residuals within the random groups and that observed values of the dependent variable bore a linear relationship to model fitted values), and all minimum adequate models satisfied these checks (a comparison of model assumptions when using non-transformed and transformed data are presented in Appendix S3).

Modeling carbon assimilation

After Medlyn et al. (2002) and Kattge and Knorr (2007), carbon assimilation was modeled using the Farquhar et al. (1980) biochemical model for perfectly coupled electron transport and the Calvin–Benson cycle, as reported in Medlyn et al. (2002). Enzyme kinetic models of photosynthesis (Farquhar et al. 1980) simulate net CO_2 assimilation (A) as the minimum of the RuBisCO-limited gross carboxylation rate (W_c) and the electron transport-limited gross carboxylation rate (W_j), scaled to account for photorespiration, minus mitochondrial (dark) respiration (R_d). The net assimilation function takes the form:

$$A = \min\{W_c, W_j\}(1 - \Gamma_*/C_i) - R_d \qquad (2)$$

where Γ_* is the CO_2 compensation point (Pa), the C_i at which the carboxylation rate is balanced by CO_2 release from oxygenation. Both W_c and W_j are modeled as functions of the intercellular CO_2 partial pressure (C_i − Pa). W_c follows a Michaelis–Menten function of C_i in which V_{cmax} (µmol CO_2 m^{-2}·s^{-1}) determines the asymptote:

$$W_c = V_{cmax} \frac{C_i}{C_i + K_c\left(1 + \frac{O_i}{K_o}\right)} \qquad (3)$$

where O_i is the intercellular O_2 partial pressure (kPa); K_c and K_o are the Michaelis–Menten constants of RuBisCO for CO_2 (Pa) and for O_2 (kPa). The light-limited gross carboxylation rate (W_j) is a function of the electron transport rate (J - µmol·e·m^{-2}·s^{-1}) following a similar function of C_i where the asymptote is proportional to J:

$$W_j = \frac{J}{4} \times \frac{C_i}{C_i + 2\Gamma_*} \qquad (4)$$

J is a function of incident photosynthetically active radiation (I – µmol photons m^{-2}·s^{-1}) that saturates at the maximum rate of electron transport (J_{max}), formulated by Harley et al. (1992) following Smith (1937), though other formulations exist:

$$J = \frac{\alpha I}{\left(1 + \left(\frac{\alpha I}{J_{max}}\right)^2\right)^{0.5}} \qquad (5)$$

where α is the apparent quantum yield of electron transport (assumed to be 0.24 mol electrons mol^{-1} photons by Harley et al. (1992) although α is not invariant in nature) and is the result of multiplying the true quantum yield and light absorption by the leaf. By determining the asymptotes of the two rate-limiting cycles of photosynthesis, it is clear from the above set of equations that carbon assimilation is highly sensitive to V_{cmax} and J_{max}.

Temperature sensitivities of V_{cmax} and J_{max} were simulated using the modified Arrhenius equation of John-

son et al. (1942), see Medlyn et al. (2002). For consistency with the temperature sensitivity functions of V_{cmax} and J_{max} (see Medlyn et al. 2002), the temperature sensitivities of the kinetic properties of RuBisCO and the CO_2 compensation point in the absence of dark respiration were modeled after Bernacchi et al. (2001). See Appendix S4 for further details.

Coefficients of the equations relating V_{cmax} to leaf N and J_{max} to V_{cmax} were taken from the models presented in Table 3. The impact of P and SLA on assimilation was simulated by predicting V_{cmax} using the 5th and 95th percentile of either P (0.05 and 0.22 mg·g^{-1}) or SLA (adjusted to provide realistic combinations of SLA and leaf N 0.01 m^2·g^{-1} and 0.025 m^2·g^{-1}) from our database. The biophysical space over which carbon assimilation was simulated was PAR ranging from 0 to 1500 μmol·m^{-2}·s^{-1}, internal CO_2 partial pressure of 30 Pa, at two levels of leaf N (0.5 and 3 g·m^{-2}) and at a temperature of 25°C.

To simulate the sensitivity of carbon assimilation to the J_{max} to V_{cmax} slope, the model was driven with a full range of photosynthetically active radiation (PAR, 0–1500 μmol·m^{-2}·s^{-1}) and three levels of V_{cmax} (25, 50 & 90 μmol·m^{-2}·s^{-1}). For simplicity, we only simulated the sensitivity at 25°C, acknowledging that temperature is also an important factor determining the sensitivity of assimilation to the J_{max} to V_{cmax} slope.

Results

V_{cmax} and J_{max} in relation to leaf N, leaf P, and SLA

The most likely model, that is, the minimum adequate model, when V_{cmax} was regressed on all three leaf traits together (leaf N, P, and SLA) was the model with SLA as the only explanatory variable (see Table S2). However, there were less data available for this analysis ($n = 90$, over 50% of which came from a single study), and as a consequence, the range of leaf N and SLA values were restricted compared with their range in the trivariate models discussed below. For this reason, we present no further discussion of V_{cmax} regressed on leaf N, leaf P, and SLA. For J_{max} regressed on V_{cmax}, leaf N, leaf P, and SLA, the minimum adequate model was of J_{max} regressed only on V_{cmax} and leaf P with no interaction (see Table S2). With increased range in the explanatory variables, we focus on the models with one less explanatory variable.

For V_{cmax} regressed against leaf N and either leaf P or SLA, the minimum adequate models were also the maximal models – those with both traits and their interaction (Table 2; models 1 and 2). Models of V_{cmax} regressed on leaf N and either SLA or leaf P were both highly significantly different from the null (intercept and random effects only) model ($P < 0.001$).

For V_{cmax} against leaf N and P (model 1), leaf N was a significant explanatory variable ($P = 0.003$), as was the interaction between leaf P and leaf N ($P = 0.054$), although just outside the 95% confidence level (Table 3). The AICc model selection procedure indicates that the P x N interaction was important and the response surface of V_{cmax} to leaf N and leaf P (Fig. 1) also shows the importance of leaf P in determining V_{cmax}. Leaf P modified the relationship of V_{cmax} to leaf N such that as leaf P increased, the sensitivity of V_{cmax} to leaf N increased (Fig. 1), that is, the coefficient of the interaction term was positive (Table 3). The term for leaf P alone was not significant, but was retained in the minimum adequate model to preserve marginality (see Venables and Ripley 2002).

For V_{cmax} against leaf N and P (model 2), increasing SLA increased the sensitivity of V_{cmax} to leaf N; however, the magnitude of the effect was smaller than the effect of increasing leaf P (Fig. 1). In contrast to the effect of leaf P, the effect of SLA alone was significant and was contradictory to its effect in interaction – increasing SLA decreased V_{cmax} although this effect was only clearly visible at low levels of SLA and leaf N (Fig. 1B). There were few data points at low SLA and low leaf N because as SLA decreases, leaf N concentrations would have to be extremely low to allow low values of leaf N when expressed on an area basis, again suggesting that the effect of SLA on V_{cmax} was not substantial.

Leaf P had a larger effect on the V_{cmax} to leaf N relationship than did SLA (compare Fig. 1A and B), by contrast SLA was more significant in model 2 than was leaf P in model 1. The contrast arises from the reduced sample size of the leaf P regressions (110 observations in eight groups) compared with the SLA regressions (260 in 20 groups). While the effect of leaf P was greater, statistical confidence in the effect was lower and more data are needed to improve our confidence in the statistical model.

For the multiple regressions of J_{max} against V_{cmax}, N, and P, the minimum adequate model was that of V_{cmax} and P, with no interaction term, explaining 84% of the residual variance compared with the null model (Table 2; model 3). For J_{max} regressed against V_{cmax}, N, and SLA, the minimum adequate model was that with V_{cmax} alone, explaining 84% of the residual variance when compared to the null model (Table 2; model 4). Both models were highly significantly different from the null model ($P < 0.001$ – Table 3). While model 4 had a slightly higher AICc than the model with V_{cmax}, SLA and their interaction as model terms (Table 2), SLA and the V_{cmax} x SLA interaction were not significant model terms ($P > 0.1$; results not shown). This was also the case for the model with V_{cmax} and SLA and this led to the selec-

Table 1. Sources of data collected for the meta-analysis and associated information including location, number of species and any experimental treatment.

Reference	Number of species	PFT*	Longitude (°E)	Latitude (°N)	Elevation (m)	Location	Country	Experiment	N	P
Aranda et al. (2005)	1	Temp Ev Bl	−3.43	39.23	650	Alburquerque	Spain	Light*water	Y	N
Bauer et al. (2001)	6	Temp Dc Bl and Ev Nl	−71.03	42.21	40	Havard forest	USA	CO$_2$*N	Y	N
Bown et al. (2007)	1	Temp Ev Nl	176.13	−38.26	600	Purokohukohu Experimental Basin	NZ	N*P	Y	Y
Brück and Guo (2006)	1	Temp legume crop	10.08	54.19	40	Kiel	Germany	NH$_4$ vs. NO$_3$	Y	N
Calfapietra (2005)	1	Temp Dc Bl	11.48	42.22	150	Viterbo	Italy	CO$_2$*N canopy level	Y	N
Carswell et al. (2005)	4	Temp Dc Bl and Ev Nl	170.3	−43.2	90	Okarito	NZ	N*P	Y	Y
Cernusak et al. (2011)	2	Trop Ev Bl	139.56	−22.59	150	Boulia	Australia	None	Y	Y
Cernusak et al. (2011)	2	"	133.19	−17.07	230	Sturt plains	Australia	None	Y	Y
Cernusak et al. (2011)	2	"	132.22	−15.15	170	Dry creek	Australia	None	Y	Y
Cernusak et al. (2011)	2	"	131.23	−14.09	70	Daly river	Australia	None	Y	Y
Cernusak et al. (2011)	2	"	131.07	−13.04	80	Adelaide river	Australia	None	Y	Y
Cernusak et al. (2011)	2	"	131.08	−12.29	40	Howard springs	Australia	None	Y	Y
Deng (2004)	2	Sub-trop forb	113.17	23.08	10	Guanzhou	China	None	Y	N
Domingues et al. (2010)	3	Trop Dc Bl	−1.5	15.34	280–300	Hombori	Mali	None	Y	Y
Domingues et al. (2010)	7	"	−1.17	12.73	250	Bissiga	Burkina Faso	None	Y	Y
Domingues et al. (2010)	8	"	−3.15	10.94	300	Dano	Burkina Faso	None	Y	Y
Domingues et al. (2010)	5	"	−1.86	9.3	370	Mole	Ghana	None	Y	Y
Domingues et al. (2010)	8	"	−1.18	7.3	170	Kogye	Ghana	None	Y	Y
Domingues et al. (2010)	21	Trop Dc Bl and Ev Bl	−1.7	7.72	200	Boabeng Fiame	Ghana	None	Y	Y
Domingues et al. (2010)	4	"	−2.45	7.14	25	Asukese	Ghana	None	Y	Y
Grassi (2002)	1	Sub-trop Ev Bl	149.07	−35.18	600	Canberra	Australia	N	Y	N
Han et al. (2008)	1	Temp Ev Nl	138.8	35.45	1030	Canberra	Australia	N	Y	N
Katahata et al. (2007)	1	Ev shrub	138.4	36.51	900	Niigata	Japan	Light*leaf age	Y	N
Kubiske (2002)	2	Temp Bl Dc	−84.04	45.33	215	Pellston	USA	N*CO$_2$*light	Y	N
Manter (2005)	1	Temp Ev Nl	−122.4	45.31	75	Portland	USA	N	Y	N
Merilo et al. (2006)	2	Temp Ev Nl	26.55	58.42	65	Saare	Estonia	Light	Y	N
Midgley et al. (1999)	4	Temp Ev shrub	20	−34.5	120	Cape Agulhas	SA	CO$_2$*N&P	Y	N
Porte and Lousteau (1998)	1	Temp Ev Nl	−0.46	44.42	60	Bordeaux	France	Leaf age*canopy level	Y	Y

Table 1. Continued.

Reference	Number of species	PFT*	Longitude (°E)	Latitude (°N)	Elevation (m)	Location	Country	Experiment	N	P
Rodriguez-Calcerrada et al. (2008)	2	Temp Dc Bl	−3.3	41.07	50	Madrid	Spain	Light	Y	N
Sholtis (2004)	1	Temp Dc Bl	−84.2	35.54	230	Oak Ridge	USA	CO_2*canopy level	Y	N
Tissue et al. (2005)	3	Temp Ev Nl and Bl Dc	170.3	−43.2	50	Okarito forest south Westland	NZ	Canopy level	Y	Y
Turnbull et al. (2007)	1	Temp Ev Bl	142.05	−37.03	470	Ballarat	Australia	Defoliation	Y	Y
Warren (2004)	1	Temp Ev Bl	143.53	−37.25	450	Creswick	Australia	N	Y	N
Watanabe et al. (2011)	1	Temp Dc Nl	141	43	180	Asapporo	Japan	CO_2*N	Y	Y
Wohlfahrt et al. (1999a)	28	Temp C3 grass and forb	11.01	46.01	1540–1900	Monte Bondone	Estern Alps	None	Y	N
Zhang and Dang (2006)	1	Temp Dc Bl	89.14	48.22	200	Ontario	Canada	CO_2*age	N	Y
Additional datasets										
TRY – Kattge et al. (2011)	1048									
Wullschleger (1993)	110									

*PFT abbreviations: Temp, temperate; Trop, tropical; Ev, evergreen; Dc, deciduous; Nl, needleleaf tree; Bl, broadleaf tree.

tion of model 4 (J_{max} against V_{cmax} alone; Tables 2 and 3) as the minimum adequate model. The inclusion of V_{cmax} in the regressions of J_{max} meant that the traits leaf N, leaf P, and SLA were tested for their effect on J_{max} that were orthogonal to their effect already implicitly considered via their effect on V_{cmax}. The leaf traits were considered as modifiers of the J_{max} to V_{cmax} relationship, not as direct determinates of J_{max}.

The effect of leaf P was significant in model 3; however, variation in leaf P had little effect on calculated values of J_{max} (Fig. 2). The effect of V_{cmax} was the most important in determining J_{max} demonstrating the tight coupling between the two maximum rate parameters. A regression of J_{max} on V_{cmax} alone yielded 301 observations, with a b_{jv} of 0.89 ± 0.02 (Table 4). In the first analysis to our knowledge of the in vivo relationship between J_{max} and V_{cmax}, Wullschleger (1993) described a slope coefficient (b_{jv}) of 1.64 for untransformed data. For comparison with our dataset, we natural-log-transformed J_{max} and V_{cmax} from the Wullschleger (1993) dataset and re-analyzed them with a linear regression. Regression assumptions were not violated by the transformation and b_{jv} was 0.84 with an R^2 of 0.87 (Table 4). In an analysis of natural-log-transformed J_{max} against V_{cmax} from the TRY database (Kattge et al. 2011), J_{max} scaled against V_{cmax} with a b_{jv} of 0.75 (and R^2 of 0.79). All three datasets have similar slope parameters for the log-transformed relationship ranging from 0.75 for the TRY data to 0.89 for our dataset (Fig. 3).

Variation in carboxylation rates caused by variation in P and SLA

The sensitivity of simulated carboxylation rates to variation in V_{cmax} and J_{max} caused by variation in leaf P or SLA (based on the minimum adequate models presented in Table 3) is shown in Fig. 4. At high leaf N (3 gm^{-2}), increasing leaf P from the 5th to the 95th percentile (0.05 gm^{-2} to 0.22 gm^{-2}) almost doubled carboxylation rates at high PAR (Fig. 4), while at low leaf N (0.5 gm^{-2}), assimilation was little affected by changes in leaf P. The increase in assimilation caused by increased leaf P at moderate-to-high leaf N, but not at low N, was because leaf P was important only in interaction with N. At low leaf P (0.05 gm^{-2}), increasing leaf N from 0.5 to 3 gm^{-2} resulted in a slight increase in carboxylation rates (compare solid lines in Fig. 4A and B). The effect of leaf P on J_{max} was so small (Table 3 and Fig. 2) in comparison with the effect of V_{cmax} that there was very little effect on carboxylation rates caused by variation in J_{max} resulting from variation in leaf P (results not shown).

Table 2. Model selection table for multiple regressions of V_{cmax} and J_{max} regressed against leaf N, or leaf N and V_{cmax} respectively, and in combination with either leaf P or SLA. The minimum adequate model (MAM) was the model with the lowest AICc. All traits were expressed on a leaf area basis and were natural-log-transformed.

Response trait	Model	Model explanatory variables[1]	Residual variance reduction (%)	AICc
V_{cmax}	Maximal model, MAM – Model 1	N, P, N:P	19.5	44.2
		N, P	16.6	45.8
		N	13.5	47.7
		P	6.5	56.9
V_{cmax}	Maximal model, MAM – Model 2	N, SLA, N:SLA	36.6	174.6
		N, SLA	32.5	185.7
		N	30.2	187.8
		SLA	12.3	248.4
J_{max}	Maximal model	V_{cmax}, N, P, all 2-way interactions, 3-way interaction	83.6	−115.6
		V_{cmax}, N, P, all 2-way interactions	83.6	−117.9
		V_{cmax}, N, P, V_{cmax}:N, N:P	83.4	−118.9
		V_{cmax}, N, P, V_{cmax}:N	83.4	−120.1
		V_{cmax}, N, P	83.4	−121.4
	MAM – Model 3	V_{cmax}, P	83.5	−123.2
		V_{cmax}, P, V_{cmax}:P	83.5	−121.2
		V_{cmax}	82.9	−120.8
		N	10.4	49.3
		P	12.5	46.2
J_{max}	Maximal model	V_{cmax}, N, SLA, all 2-way interactions, 3-way interaction	85.1	−196.2
		V_{cmax}, N, SLA, all 2-way interactions	84.7	−193.7
		V_{cmax}, N, SLA, V_{cmax}:N, V_{cmax}:SLA	84.7	−195.3
		V_{cmax}, N, SLA, V_{cmax}:SLA	84.6	−194.5
		V_{cmax}, SLA, V_{cmax}:SLA	84.5	−196.4
		V_{cmax}, SLA	84.3	−196.4
	MAM – Model 4	V_{cmax}	84.2	−196.0
		V_{cmax}, N, V_{cmax}:N	84.2	−193.0
		V_{cmax}, N	84.2	−194.0

[1]All models include an intercept term.

At high leaf N, increasing SLA from 0.01 $m^2 \cdot g^{-1}$ to 0.025 $m^2 \cdot g^{-1}$ had little effect on simulated carboxylation rates. At low leaf N (0.5 gm^{-2}), carboxylation rates were decreased as SLA increased. Assimilation was reduced at low leaf N because the effect of SLA alone (which has a negative relationship to V_{cmax}) was larger than the effect of SLA in interaction with low levels of leaf N. At higher leaf N, the effect of SLA alone was canceled by the effect of SLA in interaction with leaf N, and therefore, there was little overall effect of SLA on V_{cmax} and hence carboxylation rates (Fig. 4).

The consequence of variation in b_{jv} on carbon assimilation

To analyze the relationship of J_{max} to V_{cmax} in more depth, we investigated the effect of the slope parameter (b_{jv}) on the modeled light response of carbon assimilation at three levels of V_{cmax} (25, 50, and 90 $\mu mol \cdot m^{-2} \cdot s^{-1}$). Figure 5A–C shows the light-response curves of the W_c and W_j gross carboxylation rates. Obviously, W_c is insensitive to variation in irradiance, and W_j shows the typical saturating response at high light. Increasing b_{jv} increases the asymptote of W_j, which affects the transition point between W_c and W_j limitation. The light level at the transition where W_c and W_j are colimiting increases as b_{jv} decreases (Fig. 5A–C).

The relationship of the colimiting light level to b_{jv} allows us to categorize values of b_{jv} into two types: (1) intermediate values of b_{jv} where the point of colimitation occurs between the linear phase and the asymptote of the light response; and (2) low values at which there is no colimitation point, that is, electron transport is always limiting. Within the first category, the light level of colimitation is highly sensitive to b_{jv}. At the upper end of these intermediate b_{jv} values, the colimitation point

Table 3. Details of the recommended minimum adequate models (MAM) explaining V_{cmax} and J_{max}. All traits were expressed on an area basis and were natural-log-transformed. The LRT was the likelihood ratio test statistic of the model against the null (intercept only) model, and the residual variance reduction was the proportional reduction in residual variance when compared to the null model. A colon represents the interaction between two variables. Using the example of model 1, the equation describing V_{cmax} would take the form: $\ln(V_{cmax}) = 1.993 + 2.555\ln(N) - 0.372\ln(SLA) + 0.422\ln(N)\ln(SLA)$.

|	Response trait	Explanatory traits of the maximal model[1]	Explanatory variables of the MAM	Coefficient	SE	df	Student's *t*-test	*P*	N obs	N groups	Residual variance reduction (%)	LRT	*P*-value
Model 1	V_{cmax}	N, P	Intercept	3.946	0.229	99	17.26	<0.001	110	8	19.5	25.5	<0.001
			N	0.921	0.301	99	3.06	0.003					
			P	0.121	0.085	99	1.42	0.156					
			N:P	0.282	0.145	99	1.95	0.054					
Model 2	V_{cmax}	N, SLA	Intercept	1.993	0.410	237	4.86	<0.001	260	20	36.6	99.1	<0.001
			N	2.555	0.522	237	4.89	<0.001					
			SLA	-0.372	0.093	237	-4.00	<0.001					
			N:SLA	0.422	0.115	237	3.67	<0.001					
Model 3	J_{max}	V_{cmax}, N, P	Intercept	1.246	0.233	96	5.33	<0.001	105	7	83.5	189.1	<0.001
			V_{cmax}	0.886	0.043	96	20.60	<0.001					
			P	0.089	0.041	96	2.20	0.033					
Model 4	J_{max}	V_{cmax}, N, SLA	Intercept	1.197	0.115	215	10.45	<0.001	235	17	84.2	416.1	<0.001
			V_{cmax}	0.847	0.025	215	34.23	<0.001					

[1]Including all combinations of interactions between each trait.
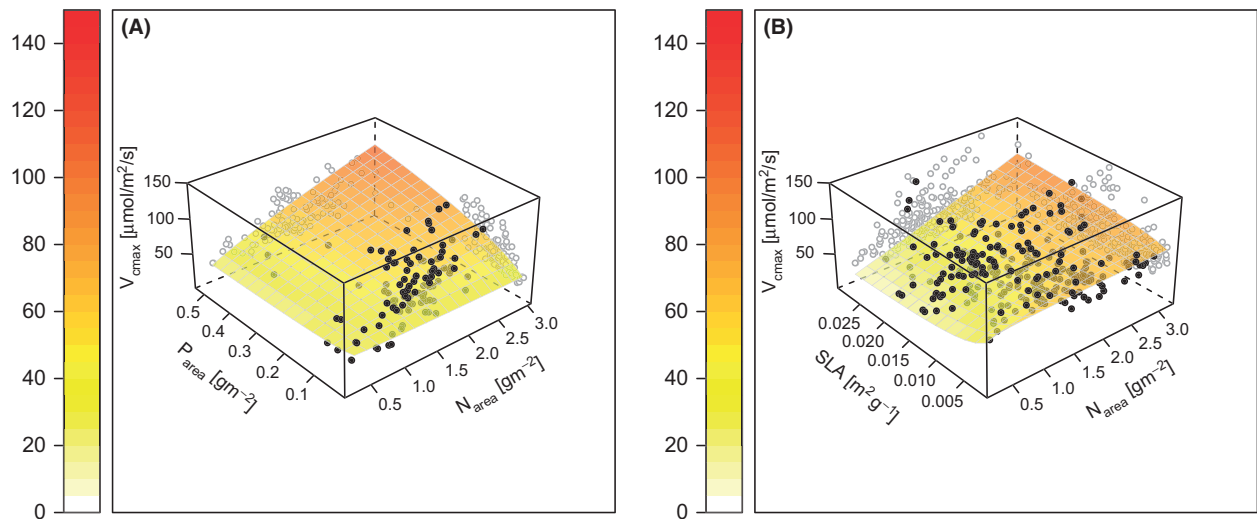
Figure 1. The derived relationships between V_{cmax} and leaf nitrogen (Table 3), as modified by leaf P (A – Table 3, model 1) and SLA (B – Table 3, model 2).

occurs while assimilation is still in the linear phase of the light response and thus maximizes quantum yield (the differential of the curve), while W_j limits photosynthesis (Fig. 5A–C). At levels of irradiance above the colimitation point, high values of b_{jv} cause W_j to be substantially higher than W_c representing "spare" electron transport capacity. As b_{jv} increases, quantum yield decreases and

the W_j asymptote approaches the W_c rate of carboxylation. In the second category of b_{jv} values, the light–response curve asymptotes below the value of W_c, that is, assimilation is light limited at all light levels, there is no colimitation, and quantum yield is very low (see Fig. 5c). It is also possible at high values of b_{jv} for the colimitation point to occur at a fixed level of irradiance, independent
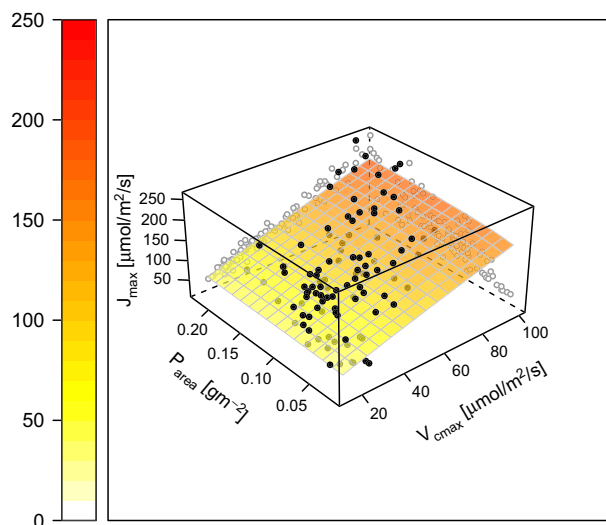
Figure 2. The relationship between J_{max} and V_{cmax} as modified by leaf P (Table 3, model 3).

of b_{jv} although these are at values of $b_{jv} > 1$ (see Fig. 5A), substantially higher than observed (Table 4).

The J_{max} to V_{cmax} relationship of the data collected in this study, and those from the TRY database (Table 4), both have values of b_{jv} within the first category (Fig. 5D–I). The transition is highly dependent on b_{jv}, and the W_c rate of assimilation is generally within the uncertainty of the potential W_j carboxylation rate at saturating light. For the coefficients derived from the data collected in this study, quantum yield is not maximized, that is, the colimitation point is never in the linear phase of the light response. When V_{cmax} was 50 $\mu mol \cdot m^{-2} \cdot s^{-1}$ and over, at light levels above those at the colimitation point, W_j was similar but slightly higher than W_c. At low photosynthetic capacity (i.e., $V_{cmax} = 25$ $\mu mol \cdot m^{-2} \cdot s^{-1}$) across the whole range of uncertainty, electron transport capacity above that necessary for carboxylation is apparent when W_c is limiting (Fig. 5D and G).
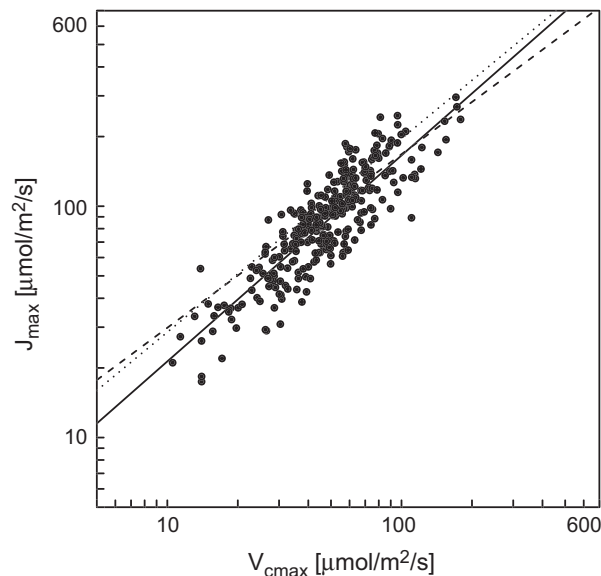
Figure 3. The relationship between J_{max} and V_{cmax} collected in this study (black circles and solid line) and compared against the regressions based on the Kattge et al. (2009) dataset (dotted line) and the Wullschleger (1993) dataset (dashed line). Log-scaled axes.

Discussion

Our goal in this study was to derive relationships of V_{cmax} and J_{max} in relation to leaf N, P, and SLA. Using a meta-analytic approach to assess patterns among 356 species drawn from 24 different studies around the world, in agreement with many previous studies, we found that V_{cmax} increased in relation to leaf N (Wohlfahrt et al. 1999b; Aranda et al. 2006; Bown et al. 2007; Kattge et al. 2009; Domingues et al. 2010) and that both leaf P and SLA increased the sensitivity of V_{cmax} to leaf N. We also found that the relationship between J_{max} and V_{cmax} was not substantially affected by leaf N, leaf P, or SLA (Table 2). Our efforts and in particular the statistical

Table 4. Slope coefficients from linear regressions of log-transformed J_{max} on V_{cmax} from the data collected in this study, from the TRY database and from Wullschleger (1993). The data collected in this study were analyzed using a mixed-effects model with the author as the random effect, while data from the other two studies were analyzed using a fixed-effects model.

	N	Model term	Coefficient	SE	Reduction in residual variance (%)	P-value*
This study	301	Intercept	1.010	0.097	86.7	<0.001
		Slope	0.890	0.021		
TRY/Kattge	1048	Intercept	1.668	0.048	78.9	<0.001
		Slope	0.750	0.012		
Wullschleger	110	Intercept	1.425	0.128	87.2	<0.001
		Slope	0.837	0.031		

*For this study's dataset, the P-value is based on the LRT statistic, and for Kattge and Wullschleger, it is based on the F statistic.
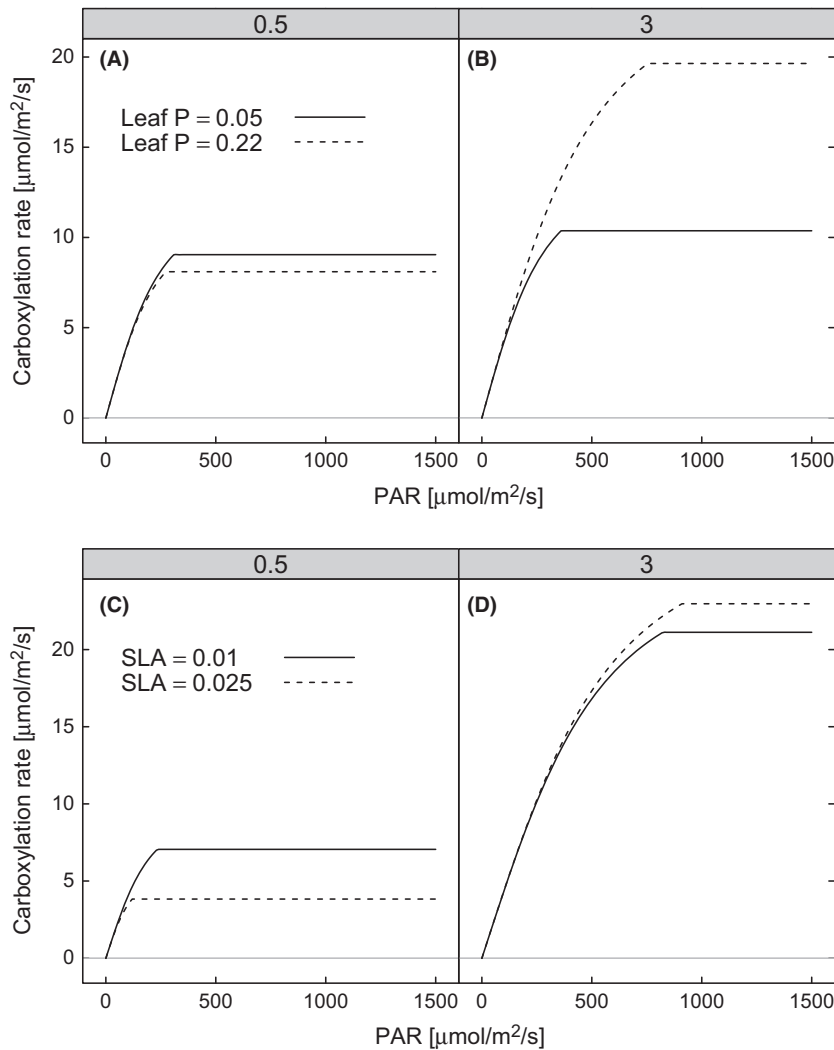
Figure 4. Simulated variation in gross carboxylation light-response curves as a result of variation in leaf P (A–B) or SLA (C–D) used in the minimum adequate models presented in Table 3. Light responses were simulated at two levels of leaf N, 0.5 gm^{-2} (A & C) and 3 gm^{-2} (B & D).

models provide a formal template on which to improve the parameterization of terrestrial ecosystem and biosphere models (TBMs; Tables 3 and 4). We demonstrated the impact of these variable rate parameters in a simple model of photosynthesis.

Evaluating the three hypotheses

In analyzing the data, we had three a priori hypotheses: (1) leaf P will modify the relationship of V_{cmax} to leaf N, (2) leaf P will modify the relationship of J_{max} to V_{cmax}, (3) the relationship between J_{max} and V_{cmax} results from a trade-off between photosynthetic gain and costs of energy dissipation.

In support of our first hypothesis, we found that leaf P was an important factor modifying the V_{cmax} to leaf N relationship. For V_{cmax}, we recommend the use in TBMs of coefficients and terms of model 1 and model 2 pre-

sented in Table 3. For those models, such as CABLE and CLM-CNP, that prognostically simulate, or explicitly parameterize leaf N and leaf P, we recommend the use of model 1 to simulate V_{cmax} (Table 3) and we suggest that incorporation of variation in leaf P is necessary for accurate scaling of V_{cmax}. Many models do not prognostically simulate SLA, and we have demonstrated that while significant, the effect size of SLA on V_{cmax} was small and we suggest it is not a priority for inclusion in TBMs for accurate parameterization of V_{cmax}. However, depending on model structure, SLA is indirectly important for scaling leaf N concentrations to area-based values of leaf N.

In contrast, and with reference to hypothesis two, we find that leaf P had little effect on the J_{max} to V_{cmax} relationship. For J_{max}, we recommend the use in TBMs and related tools of the model presented in Table 4 of J_{max} regressed on V_{cmax} alone. Although the minimum adequate model of J_{max} regressed on V_{cmax}, leaf N and P
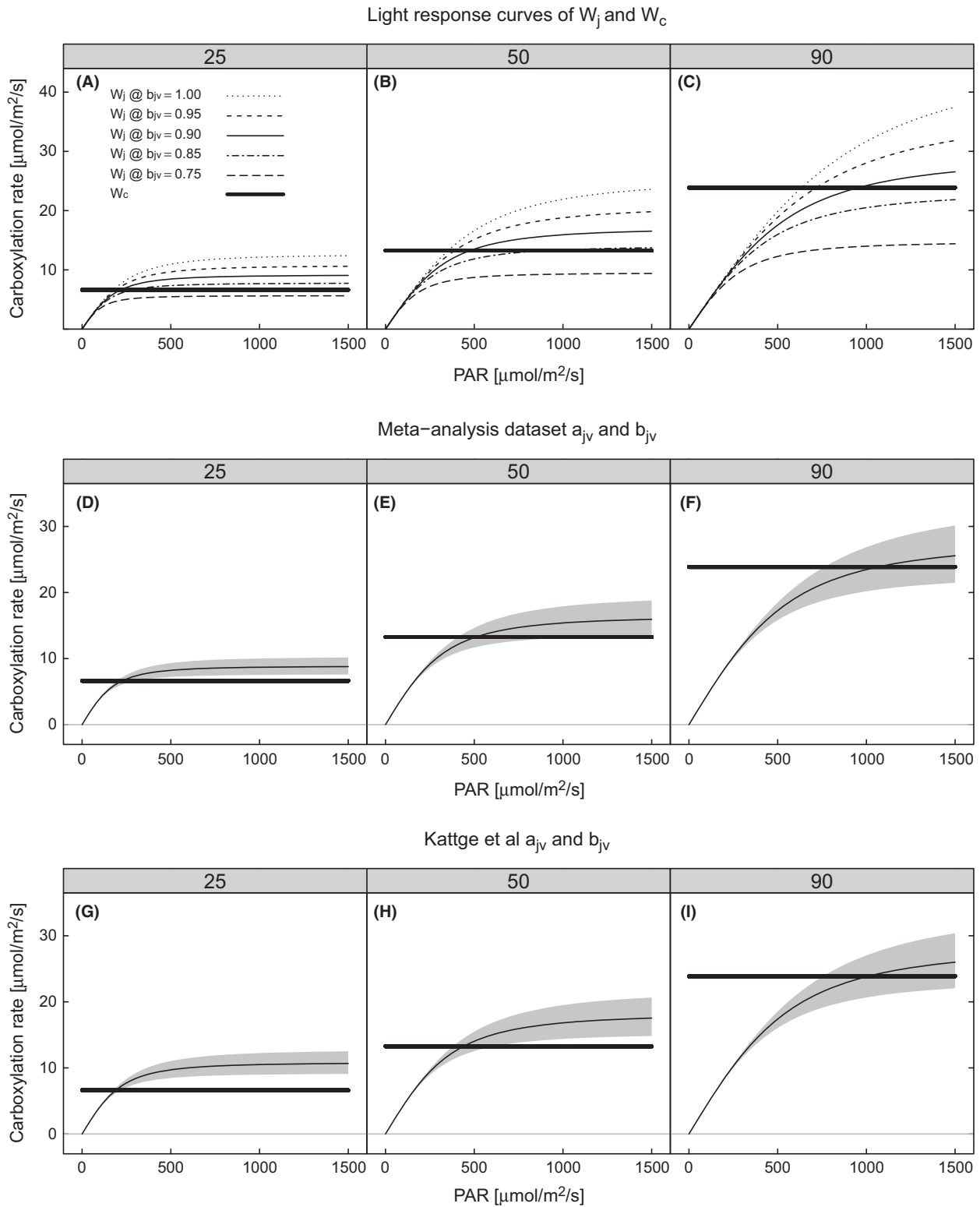
Figure 5. Simulated light-response curves of W_j and W_c in response to b_{jv} variation (A–C), using a_{jv} and b_{jv} calculated from the dataset compiled in this study (D–F) and using a_{jv} and b_{jv} calculated from the dataset of Kattge et al. (2009) (G–I). All curves calculated at three levels of V_{cmax} 25 (A, D & G), 50 (B, E & H), and 90 (C, F, & I) μmol$\cdot$m$^{-2}\cdot$s^{-1}. On panels D–I, the black line within the gray-shaded area represents W_j using the calculated coefficients and the gray-shaded area 95% confidence interval of W_j.

included leaf P as an explanatory variable, the small coefficients (Table 3) suggested that the additional impact of leaf P on J_{max} was minimal as demonstrated in Fig. 3.

The observed relationship between J_{max} and V_{cmax} run through a chloroplast-level photosynthesis model showed that the W_c rate of assimilation is generally within the uncertainty of the potential W_j carboxylation rate at saturating light and that quantum yield is not maximized. In terms of hypothesis three, the results suggest that the costs of energy dissipation and potential for photoinhibition outweigh the marginal benefits to photosynthetic gain.

The impact of leaf P

The empirical functions we present can be applied in TBMs with a phosphorus cycle and would allow scaling of V_{cmax} and J_{max} that will be more in tune with nutrient cycling than using a single parameter value for a particular plant functional type (PFT). The use of the empirical function we developed (model 1, Table 3) will reduce simulated carbon assimilation and productivity by TBMs in regions where leaf P is low and leaf N is high, and should help to improve these simulations (Mercado et al. 2011; Yang et al. 2013). Our finding for leaf P was similar to that of Reich et al. (2009) who found that, in a global analysis, increased leaf P increased the sensitivity of A_{max} to leaf N. Reich et al. (2009) showed this modification of the relationship between A_{max} and leaf N by leaf P to hold true across biomes with different N/P ratios.

The analysis of V_{cmax} and J_{max} by Domingues et al. (2010) concluded that leaf N and leaf P were best considered in terms of limiting factors, that is, that V_{cmax} was determined by either leaf N or leaf P, as often the interaction term between leaf N and P was not significant. Although within the mixed-model framework we were not able to test the limiting factor hypothesis of Domingues et al. (2010), our results suggest that aggregated across diverse sites and species, there is likely to be some colimitation between N and P.

We also aimed to ascertain whether the effect of leaf P held true across multiple biomes and whether this may be a reason for the different V_{cmax} to N sensitivities. There was some suggestion that there was an interaction of biome with the V_{cmax} relationship to N and P (results not shown), but the majority of leaf P data were gathered from within the tropical zone (Table 2) and the datasets when divided by biome were dominated by individual studies, reducing the power of the meta-analysis. In data gathered primarily within tropical latitudes, we have shown that leaf P substantially impacts the V_{cmax} to leaf N relationship.

Kattge et al. (2009) demonstrated variability in the V_{cmax} to leaf N relationship across biomes, indicating that in tropical biomes where P was expected to be more lim-

iting, V_{cmax} was less sensitive to leaf N. Our analysis shows that across a range of predominantly tropical biomes, the sensitivity of V_{cmax} to N was reduced by low leaf P and the derived relationship may help to move forward from PFT-/biome-based parameterizations in TBMs toward a trait correlation approach.

We demonstrated that variation in V_{cmax} related to variation in leaf P had a large impact on carboxylation rates. Increasing leaf P from 0.05 gm^{-2} to 0.22 gm^{-2} approximately doubled modeled gross carboxylation rates under high N levels (Fig. 4). Some of the latest generation of TBMs now includes a P cycle (Wang et al. 2010; Goll et al. 2012; Yang et al. 2013), and Mercado et al. (2011) demonstrated the importance of considering P when simulating carbon fluxes in the Amazon. In addition, anthropogenic N and P pollution has had profound effects on global ecosystems (Penuelas et al. 2012). Evidence suggests that N is more limiting than P in temperate and boreal zones (Elser et al. 2007), which may preclude the measurement of P in these zones or that studies measured P but the effects were not significant so were left out of publications. Despite a comprehensive survey of the literature, assessment of the variation in V_{cmax} in relation to the leaf N, leaf P, and SLA remains data limited. To fully quantify the effect of leaf P on the V_{cmax} to N relationship, we need more data from all ecosystems, but especially temperate and boreal ecosystems. We appeal to the leaf gas exchange research community to measure leaf P in conjunction with leaf gas exchange across all biomes.

The impact of SLA

Our results show that the relationship of V_{cmax} to leaf N was affected by SLA, albeit a small effect, at low values of leaf N (Fig. 1). Both similar and contrasting effects (Wright et al. 2004; Aranda et al. 2006) in the literature suggest that the effect of SLA on V_{cmax} is complex. SLA responds to multiple environmental and ecological factors and leaf density and leaf thickness strongly correlate with leaf N (Niinemets 1999; Poorter et al. 2009). In a previous meta-analysis, the components of SLA – leaf thickness and leaf density – showed different relationships to A_{max} (Niinemets 1999), indicating that SLA may not have a consistent effect on photosynthesis. For example, leaf thickness and leaf density are likely to have different effects on internal CO_2 conductance (g_i) and the N allocation ratio between RuBisCO and leaf structural components (Poorter et al. 2009). Unfortunately, with this dataset, we were unable to assess the effect of mesophyll conductance (g_i) on the V_{cmax} to N relationship. SLA is likely to affect g_i (Flexas et al. 2008), and the effects of SLA on the V_{cmax} to N relationship will be best assessed once when variation in g_i can be accounted for.

Resource allocation between J_{max} and V_{cmax}

The J_{max} and V_{cmax} relationship represents resource allocation between the two photosynthetic cycles – electron transport and the Calvin–Benson cycle. Coordination of resource investment in photosynthetic capacity is reflected by the strong relationship between V_{cmax} and J_{max}. Given the tight coupling of J_{max} with V_{cmax} across growth environments and species (Fig. 5), we suggest, as noted in many previous studies (Wullschleger 1993; Beerling and Quick 1995; Harley and Baldocchi 1995; Leuning 1997; Medlyn et al. 2002; Kattge and Knorr 2007), that their coupling may be a fundamental feature of plant photosynthetic trait relationships.

Traditionally, J_{max} has been related to V_{cmax} based on the assumption that optimization of resource allocation to photosynthesis would maintain a close relationship between these two parameters, an assumption verified by analysis of empirical data (e.g., Wullschleger 1993; Beerling and Quick 1995). The similarity in the regression model parameters between our dataset, the TRY dataset, and that of Wullschleger (1993) was remarkable considering the differences between these datasets (Table 4 & Fig. 3). The Wullschleger (1993) dataset comprised mainly grass and crop species as well as some temperate trees, while our dataset predominantly consists of tropical and temperate tree species.

While the general relationship between J_{max} and V_{cmax} is preserved across datasets (Fig. 3), there is substantial variation of individual species data from this relationship (Fig. 3). Some of this variation may arise due to the measurement error. V_{cmax} and J_{max} are differentially sensitive to temperature (Medlyn et al. 2002; Kattge and Knorr 2007), and their temperature sensitivity varies across species (Wohlfahrt et al. 1999b). For most species, this temperature sensitivity is not known, and while necessary, the correction of V_{cmax} and J_{max} to 25°C with non-species-specific sensitivity parameters may add variation into the J_{max} to V_{cmax} relationship. V_{cmax} is more sensitive to mesophyll conductance than J_{max} (Sun et al. 2013) and it may be that some of the variation in the relationship may be attributable to variation in g_i; however, it was not possible to determine the effect of g_i with this dataset. We present our results assuming infinite g_i because assuming infinite g_i is currently standard practice in TBMs and was the assumption made by most of the studies used in our meta-analysis. By analyzing the general relationship between J_{max} and V_{cmax}, we aim to provide a framework that can be applied to explain J_{max} to V_{cmax} relationships and consequences of variation in the relationship.

Maire et al. (2012) demonstrated that plants adjust leaf N investment to coordinate W_c and W_j (Chen et al. 1993)

for environmental conditions over the previous month (the lifetime of RuBisCO). Scaling between J_{max} and V_{cmax}, represented by the slope parameter b_{jv}, affects the light (and CO_2, Von Caemmerer and Farquhar 1981) transition point at which carbon assimilation switches between W_c and W_j, that is, the light level where W_c and W_j are colimiting. We hypothesized that b_{jv} may also coordinate instantaneous W_c and W_j when W_c is limiting as investment in J_{max} that would support rates of W_j higher than W_c, when W_c is limiting, represents investment in unused resources. At the assumed leaf absorptance and at 25°C, simulations show that potential W_j rates at high light and W_c rates are similar (Fig. 5D–I), when the probable range in b_{jv} values from our dataset (Table 4) are used. Generally, quantum yield is not maximized. Synthesized across multiple species and environments, the presented relationship suggests that J_{max} is related to V_{cmax} to coordinate W_j with W_c and hedge against photoinhibition, when RuBisCO carboxylation is limiting. Aggregated across the different species and environments, support for co-ordination at light saturation is a very general assertion. The degree of control that plants have over the relationship between J_{max} and V_{cmax} needs to be tested in controlled environments at a range of temperature and light levels (Wohlfahrt et al. 1999a) and giving consideration to mesophyll conductance and leaf absorptance.

Maire et al. (2012) show that coordination occurs over monthly timescales, while our simulations (Fig. 5) are on instantaneous timescales. The timescale over which coordination is considered is important, and given the huge diurnal variability in incident light, W_c and W_j cannot always be coordinated on subdaily timescales. The relationship that we derived between J_{max} and V_{cmax} appears to coordinate, within uncertainty bounds, the W_c and W_j rates of photosynthesis at high light levels (Fig. 5D–I). However, there is some variability and the derived relationship has high W_j at low photosynthetic capacity (Fig. 5D and G), and W_j higher than W_c when W_c is limiting indicates unused electron transport capacity at high light. Unused electron transport capacity could produce reducing power not used in carbon reduction and which could be used in biochemical pathways other than the Calvin–Benson cycle (Buckley and Adams 2011) such as the reduction of nitrite to ammonium that occurs in the chloroplast (Anderson and Done 1978; Searles and Bloom 2003) and the production of isoprene (Morfopoulos et al. 2013).

Conclusion

For the first time, we assess the sensitivity of carbon assimilation to the J_{max} to V_{cmax} relationship, and results

from the meta-analysis suggest that plants may employ a conservative strategy of J_{max} to V_{cmax} coordination to avoid photoinhibition. Work is needed to extend this analysis with the consideration of mesophyll conductance and species-specific temperature effects.

We also present for the first time the significance of P and SLA on the relationship of V_{cmax} to nitrogen and of J_{max} to V_{cmax} in a globally extensive meta-analysis. Modeling demonstrates that variation in leaf P has large consequences for carbon assimilation. The relationships presented in this study can be used to parameterize V_{cmax} and J_{max} in a rigorous fashion based on data-derived relationships, moving parameterization away from methods with limited variation or limited grounding in the literature. To fully understand variability in the relationship of V_{cmax} and J_{max} to leaf N, leaf P, and SLA, work is needed to extend the geographic range of data, particularly into temperate and boreal regions.

Acknowledgments

Conflict of Interest

None declared.

References

Anderson, J. W., and J. Done. 1978. Light-dependent assimilation of nitrite by isolated Pea chloroplasts. Plant Physiol. 61:692–697.

Aranda, X., C. Agusti, R. Joffre, and I. Fleck. 2006. Photosynthesis, growth and structural characteristics of holm oak resprouts originated from plants grown under elevated CO_2. Physiol. Plant. 128:302–312.

Atkin, O. K., M. H. M. Westbeek, M. L. Cambridge, H. Lambers, and T. L. Pons. 1997. Leaf respiration in light and darkness - A comparison of slow- and fast-growing Poa species. Plant Physiol. 113:961–965.

Bauer, G. A., G. M. Berntson, and F. A. Bazzaz. 2001. Regenerating temperate forests under elevated CO_2 and nitrogen deposition: comparing biochemical and stomatal limitation of photosynthesis. New Phytol. 152:249–266.

Beerling, D. J., and W. P. Quick. 1995. A new technique for estimating rates of carboxylation and electron-transport in leaves of C-3 plants for use in dynamic global vegetation models. Glob. Change Biol. 1:289–294.

Bernacchi, C. J., E. L. Singsaas, C. Pimentel, A. R. Portis, and S. P. Long. 2001. Improved temperature response functions for models of Rubisco-limited photosynthesis. Plant, Cell Environ. 24:253–259.

Bonan, G. B., P. J. Lawrence, K. W. Oleson, S. Levis, M. Jung, M. Reichstein, et al. 2011. Improving canopy processes in the Community Land Model version 4 (CLM4) using global flux fields empirically inferred from FLUXNET data. J. Geophys. Res. Biogeosci. 116:G02014; doi: 10.1029/2010 JG001593/abstract;jsessionid=5E06E595C92C1AEC027A49 CA8BD11601.f03t02.

Bown, H. E., M. S. Watt, P. W. Clinton, E. G. Mason, and B. Richardson. 2007. Partitioning concurrent influences of nitrogen and phosphorus supply on photosynthetic model parameters of Pinus radiata. Tree Physiol. 27:335–344.

Brück, H., and S. Guo. 2006. Influence of N form on growth photosynthesis of Phaseolus vulgaris L. plants. J. Plant Nutr. Soil Sci. 169:849–856.

Buckley, T. N., and M. A. Adams. 2011. An analytical model of non-photorespiratory CO_2 release in the light and dark in leaves of C-3 species based on stoichiometric flux balance. Plant, Cell Environ. 34:89–112.

Burnham, K. P., and D. Anderson. 2002. Model selection and multi-model inference. Springer, New York, Berlin, Heidelberg.

Cadule, P., P. Friedlingstein, L. Bopp, S. Sitch, C. D. Jones, P. Ciais, et al. 2010. Benchmarking coupled climate-carbon models against long-term atmospheric CO(2) measurements. Global Biogeochem. Cycles 24:GB2016.

Calfapietra, C., I. Tulva, E. Eensalu, M. Perez, P. De Angelis, G. Scarascia-Mugnozza, et al. 2005. Canopy profiles of photosynthetic parameters under elevated CO_2 and N fertilization in a poplar plantation. Environ. Pollut. 137:525–535.

Canadell, J. G., C. Le Quere, M. R. Raupach, C. B. Field, E. T. Buitenhuis, P. Ciais, et al. 2007. Contributions to accelerating atmospheric CO_2 growth from economic activity, carbon intensity, and efficiency of natural sinks. Proc. Natl Acad. Sci. USA 104:18866–18870.

Carswell, F. E., D. Whitehead, G. N. D. Rogers, and T. M. Mcseveny. 2005. Plasticity in photosynthetic response to nutrient supply of seedlings from a mixed conifer-angiosperm forest. Austral Ecol. 30:426–434.

Cernusak, L. A., L. B. Hutley, J. Beringer, J. A. M. Holtum, and B. L. Turner. 2011. Photosynthetic physiology of eucalypts along a sub-continental rainfall gradient in northern Australia. Agric. For. Meteorol. 151:1462–1470.

Chen, J. L., J. F. Reynolds, P. C. Harley, and J. D. Tenhunen. 1993. Coordination theory of leaf nitrogen distribution in a canopy. Oecologia 93:63–69.

Collatz, G. J., J. T. Ball, C. Grivet, and J. A. Berry. 1991. Physiological and environmental regulation of stomatal conductance, photosynthesis and transpiration - A model that includes a laminar boundary-layer. Agric. For. Meteorol. 54:107–136.

Cox, P. 2001. Hadley centre technical note 24: description of the TRIFFID dynamic global vegetation model. Hadley Centre, Met Office, Bracknell, Berks.

Deng, X., W. H. Ye, H. L. Feng, Q. H. Yang, H. L. Cao, K. Y. Hui, et al. 2004. Gas exchange characteristics of the invasive species Mikania micrantha and its indigenous congener M. cordata (Asteraceae) in South China. Bot. Bull. Acad. Sinica 45:213–220.

Domingues, T. F., P. Meir, T. R. Feldpausch, G. Saiz, E. M. Veenendaal, F. Schrodt, et al. 2010. Co-limitation of photosynthetic capacity by nitrogen and phosphorus in West Africa woodlands. Plant, Cell Environ. 33:959–980.

Elser, J. J., M. E. S. Bracken, E. E. Cleland, D. S. Gruner, W. S. Harpole, H. Hillebrand, et al. 2007. Global analysis of nitrogen and phosphorus limitation of primary producers in freshwater, marine and terrestrial ecosystems. Ecol. Lett. 10:1135–1142.

Farquhar, G. D., and S. Wong. 1984. An empirical model of stomatal conductance. Funct. Plant Biol. 11:191–210.

Farquhar, G. D., S. V. Caemmerer, and J. A. Berry. 1980. A biochemical-model of photosynthetic CO_2 assimilation in leaves of C-3 species. Planta 149:78–90.

Flexas, J., M. Ribas-Carbo, A. Diaz-Espejo, J. Galmes, and H. Medrano. 2008. Mesophyll conductance to CO_2: current knowledge and future prospects. Plant, Cell Environ. 31:602–621.

Goll, D. S., V. Brovkin, B. R. Parida, C. H. Reick, J. Kattge, P. B. Reich, et al. 2012. Nutrient limitation reduces land carbon uptake in simulations with a model of combined carbon, nitrogen and phosphorus cycling. Biogeosciences 9:3547–3569.

Grassi, G., P. Meir, R. Cromer, D. Tompkins, and P. G. Jarvis. 2002. Photosynthetic parameters in seedlings of Eucalyptus grandis as affected by rate of nitrogen supply. Plant, Cell Environ. 25:1677–1688.

Groenendijk, M., A. J. Dolman, M. K. van der Molen, R. Leuning, A. Arneth, N. Delpierre, et al. 2011. Assessing parameter variability in a photosynthesis model within and between plant functional types using global Fluxnet eddy covariance data. Agric. For. Meteorol. 151:22–38.

Gu, L., S. G. Pallardy, K. Tu, B. E. Law, and S. D. Wullschleger. 2010. Reliable estimation of biochemical parameters from C3 leaf photosynthesis–intercellular carbon dioxide response curves. Plant, Cell Environ. 33:1852–1874.

Gurevitch, J., and L. V. Hedges. 1999. Statistical issues in ecological meta-analyses. Ecology 80:1142–1149.

Han, Q., T. Kawasaki, T. Nakano, and Y. Chiba. 2008. Leaf-age effects on seasonal variability in photosynthetic parameters and its relationships with leaf mass per area and leaf nitrogen concentration within a Pinus densiflora crown. Tree Physiol. 28:551–558.

Harley, P. C., and D. D. Baldocchi. 1995. Scaling carbon dioxide and water vapour exchange from leaf to canopy in a deciduous forest. I. Leaf model parametrization. Plant, Cell Environ. 18:1146–1156.

Harley, P. C., F. Loreto, G. D. Marco, and T. D. Sharkey. 1992. Theoretical considerations when estimating the mesophyll conductance to CO_2 flux by analysis of the response of photosynthesis to CO_2. Plant Physiol. 98:1429–1436.

Johnson, F. H., H. Eyring, and R. W. Williams. 1942. The nature of enzyme inhibitions in bacterial luminescence - Sulfanilamide, urethane, temperature and pressure. J. Cell. Comp. Physiol., 20:247–268.

Katahata, S.-I., M. Naramoto, Y. Kakubari, and Y. Mukai. 2007. Photosynthetic capacity and nitrogen partitioning in foliage of the evergreen shrub Daphniphyllum humile along a natural light gradient. Tree Physiol. 27:199–208.

Kattge, J., and W. Knorr. 2007. Temperature acclimation in a biochemical model of photosynthesis: a reanalysis of data from 36 species. Plant, Cell Environ. 30:1176–1190.

Kattge, J., W. Knorr, T. Raddatz, and C. Wirth. 2009. Quantifying photosynthetic capacity and its relationship to leaf nitrogen content for global-scale terrestrial biosphere models. Glob. Change Biol. 15:976–991.

Kattge, J., S. Diaz, S. Lavorel, C. Prentice, P. Leadley, G. Boenisch, et al. 2011. TRY - a global database of plant traits. Glob. Change Biol. 17:2905–2935.

Krause, G. H., K. Winter, S. Matsubara, B. Krause, P. Jahns, A. Virgo, et al. 2012. Photosynthesis, photoprotection, and growth of shade-tolerant tropical tree seedlings under full sunlight. Photosynth. Res. 113:273–285.

Kubiske, M. E., D. R. Zak, K. S. Pregitzer, and Y. Takeuchi. 2002. Photosynthetic acclimation of overstory Populus tremuloides and understory Acer saccharum to elevated atmospheric CO_2 concentration: interactions with shade and soil nitrogen. Tree Physiol. 22:321–329.

Leuning, R. 1997. Scaling to a common temperature improves the correlation between the photosynthesis parameters J_{max} and V_{cmax}. J. Exp. Bot. 48:345–347.

Maire, V., P. Martre, J. Kattge, F. Gastal, G. Esser, S. Fontaine, et al. 2012. The coordination of leaf photosynthesis links C and N fluxes in C3 plant species. PLoS ONE 7:e38345.

Manter, D. K., K. L. Kavanagh, and C. L. Rose. 2005. Growth response of Douglas-fir seedlings to nitrogen fertilization: importance of Rubisco activation state and respiration rates. Tree Physiol. 25:1015–1021.

Marschner, H. 1995. Mineral nutrition of higher plants. Academic Press, London; San Diego.

Medlyn, B. E., E. Dreyer, D. Ellsworth, M. Forstreuter, P. C. Harley, M. U. F. Kirschbaum, et al. 2002. Temperature response of parameters of a biochemically based model of photosynthesis. II. A review of experimental data. Plant, Cell Environ. 25:1167–1179.

Mercado, L. M., S. Patino, T. F. Domingues, N. M. Fyllas, G. P. Weedon, S. Sitch, et al. 2011. Variations in Amazon forest productivity correlated with foliar nutrients and modelled rates of photosynthetic carbon supply. Philos. Trans. R. Soc. B. Biol. Sci. 366:3316–3329.

Merilo, E., K. Heinsoo, O. Kull, I. Soderbergh, T. Lundmark, and A. Koppel. 2006. Leaf photosynthetic properties in a willow (Salix viminalis and Salix dasyclados) plantation in response to fertilization. Eur. J. Forest Res. 125:93–100.

Midgley, G. F., S. J. E. Wand, and N. W. Pammenter. 1999. Nutrient and genotypic effects on CO_2-responsiveness: photosynthetic regulation in Leucadendron species of a nutrient-poor environment. J. Exp. Bot. 50:533–542.

Morfopoulos, C., I. C. Prentice, T. F. Keenan, P. Friedlingstein, B. E. Medlyn, J. Penuelas, et al. 2013. A unifying conceptual model for the environmental responses of isoprene emissions from plants. Ann. Bot. 112:1223–1238.

Niinemets, U. 1999. Components of leaf dry mass per area - thickness and density - alter leaf photosynthetic capacity in reverse directions in woody plants. New Phytol. 144:35–47.

Ordonez, J. C., P. M. van Bodegom, J.-P. M. Witte, I. J. Wright, P. B. Reich, and R. Aerts. 2009. A global study of relationships between leaf traits, climate and soil measures of nutrient fertility. Glob. Ecol. Biogeogr. 18:137–149.

Penuelas, J., J. Sardans, A. Rivas-Ubach, and I. A. Janssens. 2012. The human-induced imbalance between C, N and P in Earth's life system. Glob. Change Biol. 18:3–6.

Pinheiro, J., D. Bates, S. DebRoy, and D. Sarkar, Team RDC. 2011. *nlme: Linear and Nonlinear Mixed Effects Models*.

Poorter, H., U. Niinemets, L. Poorter, I. J. Wright, and R. Villar. 2009. Causes and consequences of variation in leaf mass per area (LMA): a meta-analysis. New Phytol. 182:565–588.

Porte, A., and D. Loustau. 1998. Variability of the photosynthetic characteristics of mature needles within the crown of a 25-year-old Pinus pinaster. Tree Physiol. 18:223–232.

Powles, S. B. 1984. Photoinhibition of photosynthesis induced by visible light. Annu. Rev. Plant Physiol. 35:15–44.

R Core Development Team. 2011. R: A language and environment for statistical computing. R Foundation for Statistical Computing, Vienna.

Reich, P. B., J. Oleksyn, and I. J. Wright. 2009. Leaf phosphorus influences the photosynthesis-nitrogen relation: a cross-biome analysis of 314 species. Oecologia 160:207–212.

Rodriguez-Calcerrada, J., P. B. Reich, E. Rosenqvist, J. A. Pardos, F. J. Cano, and I. Aranda. 2008. Leaf physiological versus morphological acclimation to high-light exposure at different stages of foliar development in oak. Tree Physiol. 28:761–771.

Rogers, A. 2014. The use and misuse of Vcmax in earth system models. Photosynth. Res. 119:15–29.

Searles, P. S., and A. J. Bloom. 2003. Nitrate photo-assimilation in tomato leaves under short-term exposure to elevated carbon dioxide and low oxygen. Plant, Cell Environ. 26:1247–1255.

Sharkey, T. D., C. J. Bernacchi, G. D. Farquhar, and E. L. Singsaas. 2007. Fitting photosynthetic carbon dioxide response curves for C3 leaves. Plant, Cell Environ. 30:1035–1040.

Sholtis, J. D., C. A. Gunderson, R. J. Norby, and D. T. Tissue. 2004. Persistent stimulation of photosynthesis by elevated CO_2 in a sweetgum (Liquidambar styraciflua) forest stand. New Phytol. 162:343–354.

Sitch, S., B. Smith, I. C. Prentice, A. Arneth, A. Bondeau, W. Cramer, et al. 2003. Evaluation of ecosystem dynamics, plant geography and terrestrial carbon cycling in the LPJ dynamic global vegetation model. Glob. Change Biol. 9:161–185.

Smith, E. L. 1937. The influence of light and carbon dioxide on photosynthesis. J. Gen. Physiol. 20:807–830.

Software, D.. 2008. Grab it!. Datatrend Software, Raleigh, NC USA.

Sun, Y., L. Gu, R. E. Dickinson, S. G. Pallardy, J. Baker, Y. Cao, et al. 2013. Asymmetrical effects of mesophyll conductance on fundamental photosynthetic parameters and their relationships estimated from leaf gas exchange measurements. Plant, Cell Environ. 978–994.

Taiz, L., and E. Zeiger. 2010. Plant physiology. Sinauer Assoc, Sunderland, Mass.

Tissue, D. T., K. L. Griffin, M. H. Turnbull, and D. Whitehead. 2005. Stomatal and non-stomatal limitations to photosynthesis in four tree species in a temperate rainforest dominated by Dacrydium cupressinum in New Zealand. Tree Physiol. 25:447–456.

Turnbull, T. L., M. A. Adams, and C. R. Warren. 2007. Increased photosynthesis following partial defoliation of field-grown Eucalyptus globulus seedlings is not caused by increased leaf nitrogen. Tree Physiol. 27:1481–1492.

Venables, W. N., and B. D. Ripley. 2002. Modern applied statistics with S. Springer, New York.

Verheijen, L. M., V. Brovkin, R. Aerts, G. Bönisch, J. H. C. Cornelissen, J. Kattge, et al. 2012. Impacts of trait variation through observed trait-climate relationships on performance of a representative earth system model: a conceptual analysis. Biogeosci. Discuss. 9:18907–18950.

Von Caemmerer, S., and G. D. Farquhar. 1981. Some relationships between the biochemistry of photosynthesis and the gas exchange of leaves. Planta 153:376–387.

Wang, Y. P., R. M. Law, and B. Pak. 2010. A global model of carbon, nitrogen and phosphorus cycles for the terrestrial biosphere. Biogeosciences 7:2261–2282.

Warren, C. R. 2004. The photosynthetic limitation posed by internal conductance to CO_2 movement is increased by nutrient supply. J. Exp. Bot. 55:2313–2321.

Watanabe, M., Y. Watanabe, S. Kitaoka, H. Utsugi, K. Kita, and T. Koike. 2011. Growth and photosynthetic traits of hybrid larch F1 (Larix gmelinii var. japonica × L. kaempferi) under elevated CO_2 concentration with low nutrient availability. Tree Physiol. 31:965–975.

Wohlfahrt, G., M. Bahn, and A. Cernusca. 1999a. The use of the ratio between the photosynthesis parameters Pml and V_{cmax} for scaling up photosynthesis of C3 plants from leaves to canopies: a critical examination of different modelling approaches. J. Theor. Biol. 200:163–181.

Wohlfahrt, G., M. Bahn, E. Haubner, I. Horak, W. Michaeler, K. Rottmar, et al. 1999b. Inter-specific variation of the biochemical limitation to photosynthesis and related leaf traits of 30 species from mountain grassland ecosystems under different land use. Plant, Cell Environ. 22:1281–1296.

Woodward, F. I., T. M. Smith, and W. R. Emanuel. 1995. A global land primary productivity and phytogeography model. Global Biogeochem. Cycles 9:471–490.

Wright, I. J., P. B. Reich, M. Westoby, D. D. Ackerly, Z. Baruch, F. Bongers, et al. 2004. The worldwide leaf economics spectrum. Nature 428:821–827.

Wullschleger, S. D. 1993. Biochemical limitations to carbon assimilation in C3 plants - a retrospective analysis of the A/Ci curves from 109 species. J. Exp. Bot. 44:907–920.

Xu, R. 2003. Measuring explained variation in linear mixed effects models. Stat. Med. 22:3527–3541.

Yang, X., P. E. Thornton, D. M. Ricciuto, and W. M. Post. 2013. The role of phosphorus dynamics in tropical forests – a modeling study using CLM-CNP. Biogeosci. Discuss. 10:14439–14473.

Zaehle, S., and A. D. Friend. 2010. Carbon and nitrogen cycle dynamics in the O-CN land surface model: 1. Model description, site-scale evaluation, and sensitivity to parameter estimates. Global Biogeochem. Cycles 24:GB1005.

Zaehle, S., S. Sitch, B. Smith, and F. Hatterman. 2005. Effects of parameter uncertainties on the modeling of terrestrial biosphere dynamics. Global Biogeochem. Cycles 19:GB3020.

Zhang, S., and Q.-L. Dang. 2006. Effects of carbon dioxide concentration and nutrition on photosynthetic functions of white birch seedlings. Tree Physiol. 26:1457–1467.

Supporting Information

Additional Supporting Information may be found in the online version of this article:

Appendix S1

Table S1. Species that feature in the meta-analysis

Table S2. Model selection table for multiple regressions of V_{cmax} and J_{max} regressed against leaf N, P and SLA, or leaf N, P, SLA and V_{cmax} respectively. The minimum adequate model (MAM) was the model with the lowest AICc. All traits were expressed on a leaf area basis and were natural log transformed.

Appendix S2. Standardisation of V_{cmax} and J_{max} to common kinetic parameters and photosynthetic functions.

Figure S1. Original and standardised values of V_{cmax} and J_{max} both expressed at $25°C$.

Figure S2. Standardised values of V_{cmax} and J_{max} (both expressed at $25°C$) using Eq 9 to calculate Γ_* using O_i assumed by the authors of the original publication (20–21 kPa; *x*-axis) and an assumed reduction in O_i with altitude (*y*-axis).

Appendix S3. Model assumptions and selection

Table S3. Model selection table for multiple regressions of V_{cmax} and J_{max} regressed against leaf N, P and SLA, or leaf N, P, SLA and V_{cmax} respectively.

Figure S3. Plots of the mixed-model regression assumptions for the un-transformed J_{max} to V_{cmax} relationship for the data collected in this study.

Figure S4. Plots of the mixed-model regression assumptions for the transformed J_{max} to V_{cmax} relationship for the data collected in this study.

Appendix 4. Modelling photosynthesis.